BJP British Journal of Pharmacology

DOI:10.1111/bph.12831
www.brjpharmacol.org

RESEARCH PAPER

Different apoptotic effects of [Pt(*O,O′*-acac)(γ-acac)(DMS)] and cisplatin on normal and cancerous human epithelial breast cells in primary culture

Carla Vetrugno[1,*], Antonella Muscella[2,*], Francesco Paolo Fanizzi[3], Luca Giulio Cossa[1], Danilo Migoni[3], Sandra Angelica De Pascali[3] and Santo Marsigliante[1]

[1]*Cell Physiology Lab,* [2]*Cell Pathology Lab, and* [3]*General and Inorganic Chemistry Lab, Dipartimento di Scienze e Tecnologie Biologiche e Ambientali (Di.S.Te.B.A.), Universita' del Salento, Lecce, Italy*

Correspondence
Santo Marsigliante, Cell Physiology Lab, Dipartimento di Scienze e Tecnologie Biologiche e Ambientali (Di.S.Te.B.A.), Universita' del Salento, Lecce, Italy. E-mail: santo.marsigliante@unisalento.it

*These two authors equally contributed to this work (Vetrugno, Muscella).

Received
4 December 2013
Revised
16 June 2014
Accepted
24 June 2014

BACKGROUND AND PURPOSE

The aim of this study was to determine whether [platinum (Pt)(*O,O′*-acetylacetonate (acac))(γ-acac)(dimethylsulphide (DMS))] is differentially cytotoxic in normal and cancer cells, and to measure comparative levels of cytotoxicity compared with cisplatin in the same cells.

EXPERIMENTAL APPROACH

We performed experiments on cancerous and normal epithelial breast cells in primary culture obtained from the same patients. The apoptotic effects [Pt(*O,O′*-acac)(γ-acac)(DMS)] and cisplatin in cancerous and normal breast cells were compared.

KEY RESULTS

Cancer cells were more sensitive to [Pt(*O,O′*-acac)(γ-acac)(DMS)] (IC_{50} = 5.22 ± 1.2 μmol·L^{-1}) than normal cells (IC_{50} = 116.9 ± 8.8 μmol·L^{-1}). However, the difference was less strong when cisplatin was used (IC_{50} = 96.0 ± 6.9 and 61.9 ± 6.1 μmol·L^{-1} for cancer and normal cells respectively). Both compounds caused reactive oxygen species (ROS) production with different mechanisms: [Pt(*O,O′*-acac)(γ-acac)(DMS)] quickly activated NAD(P)H oxidase while cisplatin caused a slower formation of mitochondrial ROS. Cisplatin and [Pt(*O,O′*-acac)(γ-acac)(DMS)] caused activation of caspases, proteolysis of PARP and modulation of Bcl-2, Bax and Bid. [Pt(*O,O′*-acac)(γ-acac)(DMS)] also caused leakage of cytochrome c from the mitochondria. Overall, these processes proceeded more quickly in cells treated with [Pt(*O,O′*-acac)(γ-acac)(DMS)] compared with cisplatin. [Pt(*O,O′*-acac)(γ-acac)(DMS)] effects were faster and quantitatively greater in cancer than in normal cells. [Pt(*O,O′*-acac)(γ-acac)(DMS)] caused a fast decrease of mitochondrial membrane potential, especially in cancer cells.

CONCLUSIONS AND IMPLICATIONS

[Pt(*O,O′*-acac)(γ-acac)(DMS)] was specific to breast cancer cells in primary culture, and this observation makes this compound potentially more interesting than cisplatin.

Abbreviations

DMS, dimethylsulphide; NBT, nitroblue tetrazolium; ROS, reactive oxygen species; SRB, sulforhodamine B

© 2014 The British Pharmacological Society

Table of Links

TARGETS	LIGANDS
Bid	Cisplatin
Caspases	

This Table lists key protein targets and ligands in this article which are hyperlinked to corresponding entries in http://www.guidetopharmacology.org, the common portal for data from the IUPHAR/BPS Guide to PHARMACOLOGY (Pawson *et al.*, 2014) and are permanently archived in the Concise Guide to PHARMACOLOGY 2013/14 (Alexander *et al.*, 2013).

Introduction

Breast cancer is the second most common cause of death by cancer in women (Ferlay *et al.*, 2010). Breast cancer is a heterogeneous disease consisting of a variety of subtypes that needs different treatment strategies.

Cisplatin is a well-known DNA-damaging agent and DNA platination is an essential first step in the cytotoxic activity of the drug (Fuertes *et al.*, 2003). DNA damage is a classical inducer of p53 function, a protein either involved in apoptosis or DNA repair depending on the cellular types (Strasser *et al.*, 1994). Cisplatin is widely used for the treatment of many malignancies, including breast, testicular, ovarian, bladder, cervical, head and neck, and small cell and non-small cell lung (Gandara *et al.*, 1989; Smith and Talbot, 1992). Despite its success, the clinical usefulness of cisplatin is limited by its severe side effects such as dose-dependent nephrotoxicity, nausea, vomiting, ototoxicity, neurotoxicity and myelo-suppression (Fuertes *et al.*, 2003). Modification of platinum (Pt)-based compounds is a promising approach for the development of non cross-resistant analogues of cisplatin and a large number of mononuclear Pt compounds have been developed as potential candidates for clinical use (Farrell, 1996). In this context, new Pt(II) complexes used in the present study have been specifically synthesized by some of us to overcome the cisplatin related problems (De Pascali *et al.*, 2005; 2009). The ability of these new compounds to induce apoptosis in human cancer cells has been studied and compared with the well-established anticancer drug, cisplatin. Among all anticancer compounds available, [Pt(*O,O′*-acac)(γ-acac)(DMS)] exhibited the highest *in vitro* activity (Muscella *et al.*, 2007; 2008; 2011a,b). The reactivity of these novel complexes with nucleobases and sulphur ligands suggests that their cytotoxicity may not necessarily due to an interaction with DNA (De Pascali *et al.*, 2005). [Pt(*O,O′*-acac)(γ-acac)(DMS)] passes the blood–brain barrier and reaches the CNS in doses much higher than cisplatin, but displays a low neurotoxicity in normal tissues (Cerri *et al.*, 2011). Our results show that [Pt(O,O′-acac)(γ-acac)(DMS)] exhibited higher anti-tumour activity than cisplatin *in vitro* on MCF-7 and in other breast cancer cell lines, but not in MCF-10A cells, which are considered to be normal and non-cancerous breast cells (Muscella *et al.*, 2008).

In order to determine if [Pt(O,O′-acac)(γ-acac)(DMS)] was specifically toxic for cancer cells, we studied its effects in primary cultured epithelial breast cells obtained from 30 tumour tissues. Results were compared with those achieved in primary cultured epithelial breast cells obtained from the corresponding histologically proven non-malignant tissue adjacent to the tumour. This allowed us to specifically evaluate the responsiveness of the cell types obtained from the same patients. Our results confirm that [Pt(*O,O′*-acac)(γ-acac)(DMS)] is also more potent than cisplatin in primary culture and displays a higher cytotoxic activity in epithelial breast cancer cells in primary culture, than in normal cells. Results indicate that this new Pt-complex may be a potential novel anti-tumour agent.

Methods

Primary culture of breast epithelial cells

Thirty breast cancer tissues and corresponding histologically proven non-malignant tissue adjacent to the tumour were obtained after surgery performed in the 'Vito Fazzi' hospital. All patients gave informed consent to study participation before enrolment. All the tumours were invasive intraductal carcinomas from patients who fulfilled the following inclusion criteria: having a breast lesion pathologically diagnosed as malignant by core biopsy, had not received any therapy before surgery, were not pregnant at the time of diagnosis and with no history of breast cancer or previous breast surgery including breast implants.

Portions of tissue were immediately sent to the histopathology laboratory for the histological diagnosis. Other portions were placed into transport medium and disaggregated immediately, as described previously (Greco *et al.*, 2002). Twenty-six out of 30 were oestrogen (ER)-positive tumours, 25/30 were ER-positive/progesterone (PgR)-positive tumours and only one tumour was triple negative.

Cultured cells exhibited the characteristic features of epithelial cells that is a positive immunocytochemical staining for cytokeratin 19. Contamination from fibroblasts was quantified using anti-vimentin antibody (Sigma, Milan, Italy). Their expression was lower than 5%.

In all experiments, normal and corresponding tumour breast epithelial cells were used in primary culture at passages 2 and 3 because the ER and PgR concentrations (specific markers of the epithelial source of the breast cells) remained stable until the third or fourth passage.

We were forced to perform our experiments on different groups of normal and cancer pairs randomly chosen, as specified later, because the amount of material that would have been needed was not available due to the necessity to limit our use of cultured cells to the second and third passages.

Enzyme immunoassay (EIA) of ER and PgR receptors

EIAs for ER and PgR (Abbott, Chicago, IL, USA) were carried out in accordance with the manufacturer's instructions.

Cytotoxicity assay

We evaluated the IC_{50} in all pairs of cultures (n = 30 normal/cancer pairs) with 3-(4,5-dimethylthiazol-2-yl)-2,5-diphenol tetrazolium bromide (MTT) and sulforhodamine B (SRB) assays. The SRB assay and the conversion of MTT by breast cells were used as an indicator of cell number, as described previously (Muscella *et al.*, 2008). The percentage of survival was calculated as the absorbance ratio of treated to untreated cells. Viable cells were also counted by the Trypan blue exclusion assay and light microscopy. The data presented are means ± SD from eight replicate wells per microtitre plate.

Pt determination

The Pt content was determined on a group of five normal and cancer pairs (from the same patients) randomly chosen. To determine total Pt content, cells (each experimental point consisted of approximately 1.5 million cells) were washed twice in 0.9% NaCl solution and then digested in 0.5 mL of 65% nitric acid by incubation at 37°C for at least 2 days to obtain a clear solution.

To determine Pt content in distinct subcellular fractions, cytosolic, nuclear and DNA extracts were digested in 65% nitric acid solution by incubation at 37°C for at least 2 days to obtain a clear solution. Pt content in the samples was determined by inductively coupled plasma atomic emission spectroscopy (ICP-AES) spectrometry on an iCAP 6000 Thermo Scientific spectrometer (Waltham, MA, USA). The reproducibility of measurements, linearity of calibration curve and low limit of detection demonstrated in preliminary studies proved that this method is sensitive and accurate and therefore suitable for determination of Pt content in cells (Muscella *et al.*, 2007). All measurements were performed in triplicate and included three quality controls according to standard operating procedures. The cellular Pt levels were expressed as ng of Pt per mg of protein or as pg of Pt per mg of DNA. Data were obtained from four independent experiments with duplicate cultures.

Reactive oxygen species (ROS) measurements

Experiments on ROS generation were made on five randomly chosen normal and cancer pairs (obtained from the same patients). ROS generation was detected by nitroblue tetrazolium (NBT) assay as previously described (Muscella *et al.*, 2010). Briefly, NBT (1 mg·mL^{-1}) was added to the medium of cells and incubations were carried out at 37°C for 30 min. Cells were then washed and lysed in a 90% DMSO solution containing 0.01 N NaOH and 0.1% SDS. Absorbance was measured at 550 nm against lysis buffer blank. Data are expressed as percentage of control untreated cells.

Spectroscopic analysis of mitochondrial membrane depolarization

Mitochondrial membrane depolarization experiments were made on five randomly chosen normal and cancer pairs (obtained from the same patients). Mitochondrial membrane depolarization was detected by a shift in fluorescence emission (EM) of the lipophilic cationic probe 5,5′,6,6′-tetrachloro-1,1′,3,3′-tetraethylbenzimidazolo-carbocyanine iodide (JC-1). JC-1 is able to enter mitochondria selectively, where it exists as a J-aggregate, emitting at 590 nm (red/yellow) after excitation (EX) at 488 nm (Smiley *et al.*, 1991). Changes in the mitochondrial membrane potential ($\Delta\Psi_m$) and subsequent depolarization result in dissociation of the aggregate into the monomeric form of the dye, causing a shift in EM to 530 nm (green), which can be detected (Smiley *et al.*, 1991).

The uptake of JC-1 and the formation of J-aggregates by breast cells were monitored by fluorescent spectrophotometry. Inside the mitochondria, the fluorescence EM shifts from green (monomers of JC-1) to red (aggregates). The shifts were detected fluorimetrically (using EX 490 nm and EM 590 nm for red, and 525 nm for green) using a JASCO FP 750 fluorimeter (JASCO Corporation, Tokyo, Japan). Mitochondrial depolarization is indicated by a decrease in the red to green fluorescence ratio. Preliminary experiments demonstrated that under these conditions, the dye reached near equilibrium distribution and gave a maximal fluorescence response to a fall in ΔΨm induced by the mitochondrial uncoupler carbonylcyanide-m-chloro-phenyl-hydrazone (5 μmol·L^{-1}).

Superoxide anion (O_2^-) production

Superoxide anion production assay was performed on the same five normal and cancer pairs (obtained from the same patients) used to make the determination of the mitochondrial membrane depolarization. O_2^- is the main free radical produced in the mitochondria and was measured in breast cells using the cell-permeable probe MitoSOX Red as previously described (Muscella *et al.*, 2011a,b). The fluorescence intensity was measured with a JASCO FP 750 fluorimeter. EX monochromators were set at 488 nm, with a chopper interval of 0.5 s, and the EM monochromator was set at 580 nm.

Preparation of subcellular fraction

To obtain protein cell extracts, cells were washed twice in ice-cold PBS and harvested in 1 mL of PBS. The samples were centrifuged for 30 s at 10 000× g, and cell pellets were resuspended in the following buffer (mmol·L^{-1}): 20 Tris–HCl (pH 8.0) containing 100 NaCl, 2 EDTA, 2 Na_3VO_4, 0.2% Nonidet P-40 and 10% glycerol, supplemented with a cocktail of protease inhibitors (1 mg·mL^{-1} of each of the proteinase inhibitors aprotinin, leupeptin, soybean trypsin inhibitor, and 1 mmol·L^{-1} phenylmethylsulphonyl fluoride, all from Sigma). After a 10 min incubation on ice, the cells were passed several times through a 20-gauge needle, and then centrifuged at 13 000× g for 10 min at 4°C. For preparation of subcellular fractions, the cells were ruptured in homogenization buffer (mmol·L^{-1}): 20 Tris–HCl (pH 7.5) containing 250 sucrose, 2 EDTA, 0.5 EGTA, 0.2 phenylmethylsulphonyl

fluoride and the cocktail of protease inhibitors, by Dounce homogenization, and centrifuged immediately at 2000× *g* for 10 min. The supernatant was collected and centrifuged at 100 000× *g* for 1 h to separate cytosolic and membrane fractions. The membrane fraction was subsequently resuspended in extraction buffer (mmol·L^{-1}): 20 Tris–HCl (pH 7.5) containing 150 NaCl, 1 EDTA, 1 EGTA, 0.2 phenylmethylsulphonyl fluoride and the cocktail of protease inhibitors with 1% (v/v) Nonidet P-40. Nuclei were pelleted by centrifugation at 2000× *g* for 15 min at 4°C, and resuspended in high-salt buffer (mmol·L^{-1}): 20 Tris–HCl (pH 7.9), 420 NaCl, 10 KCl, 0.1 Na_3VO_4, 1 EDTA, 1 EGTA, 20% glycerol, supplemented with a cocktail of protease inhibitors, and sonicated until no nuclei remained intact. The samples were then centrifuged at 13 000× *g* for 10 min at 4°C, and the resultant supernatant was used as the nuclear extract.

For the preparation of mitochondrial and cytosolic proteins cells were trypsinized and washed once with ice-cold PBS and gently lysed for 30 s in 80 mL ice-cold lysis buffer [250 mmol·L^{-1} sucrose, 1 mmol·L^{-1} EDTA, 0.05% digitonin, 25 mmol·L^{-1} Tris (pH 6.8), 1 mmol·L^{-1} dithiothreitol and the cocktail of protease inhibitors]. The lysate was centrifuged at 12 000× *g* at 4°C for 3 min to separate the supernatant (mitochondria-free cytosolic extract) and the pellet (mitochondria-containing fraction). Supernatant (40 µg) and pellet (40 µg) were subjected individually to SDS–PAGE.

The purity of fractions was tested by immunoblotting with anti α subunit of Na^+/K^+-ATPase monoclonal antibody (membrane protein), anti-histone-3/4 polyclonal antibody (nuclear proteins), β-actin (cytoplasmic protein) or porin (mitochondrial membrane protein). Proteins in the homogenates and cellular fraction were determined using the Bio-Rad (Milan, Italy) protein assay kit 1. Lyophilized BSA was used as a standard.

Western blot analysis

Western blots for caspases, PARP, Bid, Bax and Bcl-2 were made on five randomly chosen normal and cancer pairs (obtained from the same patients) and each experimental point consisted of approximately 600 000 cells. Proteins in homogenates and cellular fraction were determined using the Bio-Rad protein assay kit 1. Lyophilized BSA was used as a standard. Total cell proteins or proteins of the distinct subcellular fractions were dissolved in SDS sample buffer and separated on 10 or 15% SDS gels. Separated proteins were transferred electrophoretically onto the PVDF membrane (Amersham International, Piscataway, NJ, USA). Equal protein loading was confirmed by Ponceau S staining. Blots were incubated with specific primary antibodies, and the immune complexes were detected using appropriate peroxidase conjugated secondary antibodies and enhanced chemiluminescent detection reagent enhanced chemiluminescence (Amersham International). The blots were stripped and used for sequential incubation with control antibodies. Densitometric analysis was carried out on the Western blots using the NIH Image (v1.63) software (National Institutes of Health, Bethesda, MD, USA). The pixel intensity for each region was analysed, the background was subtracted and the protein expressions were normalized to β-actin loading control for each lane.

Data analysis

Results are shown as means ± SD. Statistical analysis was carried out using ANOVA and, as indicated, *post hoc* tests (Bonferroni or Dunn) were also performed. Differences between groups were tested using Student's *t*-test. A *P* value less than 0.05 were considered to achieve statistical significance.

Materials

RPMI 1640 medium, antibiotics, glutamine and FBS were purchased from Celbio (Pero, MI, Italy). Caspase-7, -9 and -3, Bax, Bid, PARP, Bcl-2, were obtained from Cell Signalling Technology (Celbio, Milan, Italy).

Anti-porin (or anti-voltage-dependent anion selective channel 1), goat anti-rabbit conjugated with peroxidase and control antibodies, were obtained from Santa Cruz Biotechnology, Inc. (Sta. Cruz, CA, USA). All others reagents were from Sigma.

Results

Cytotoxicity of the drugs

Cells were treated with various concentrations of [Pt(*O,O′*-acac)(γ-acac)(DMS)] or cisplatin, and viable cell number was determined by MTT metabolic assay and confirmed by SRB assay 12, 24, 48 and 72 h later. As comparable results were also obtained when the cell number was directly determined by cell counting, the MTT assay was used in the experiments described hereafter. Both [Pt(*O,O′*-acac)(γ-acac)(DMS)] and cisplatin provoked a dose-dependent decrease in cell survival at different extent. In breast cancer cells [Pt(O,O′-acac)(γ-acac)(DMS)] cytotoxicity was approximately 18-fold greater than that observed for cisplatin (IC_{50} 5.22 ± 1.2 µmol·L^{-1} for [Pt(O,O′-acac)(γ-acac)(DMS)] and IC_{50} 96.0 ± 6.9 µmol·L^{-1} for cisplatin; $P < 0.0001$, after 72 h treatment, $n = 30$ primary cultures). Conversely, in non-cancerous cells obtained from non-malignant tissue adjacent to the tumour, cisplatin was significantly more cytotoxic than [Pt(O,O′-acac)(γ-acac)(DMS)] (IC_{50} 116.9 ± 8.8 µmol·L^{-1} for [Pt(*O,O′*-acac)(γ-acac)(DMS)] and IC_{50} 61.9 ± 6.1 µmol·L^{-1} for *cisPt*; $P < 0.001$, after 72 h treatment, $n = 30$ primary cultures). Epithelial breast cancer cells were therefore more sensitive to [Pt(*O,O′*-acac)(γ-acac)(DMS)] than normal cells, while results were opposite when cisplatin was used (Table 1 shows IC_{50} obtained in all primary cell cultures used). Cells were also continuously exposed to 10 and 100 µmol·L^{-1} of cisplatin or to [Pt(*O,O′*-acac)(γ-acac)(DMS)] and cell viability was monitored by MTT assay over a period of 72 h (Figure 1A–D).

Accumulation of [Pt(O,O′-acac)(γ-acac)(DMS)] and cisplatin in cells

Cellular accumulation measurements showed that [Pt(*O,O′*-acac)(γ-acac)(DMS)] and cisplatin accumulated proportionally to the concentration of the drug up to 100 µmol·L^{-1} in a linear fashion (Figure 2A and B). This indicates that there is no saturation of the uptake of either drug at concentrations in this range. [Pt(*O,O′*-acac)(γ-acac)(DMS)] concentration in both normal and cancerous cells increased rapidly and reached the maximum level after 6 h, at which point its

Table 1

IC_{50} values after a 72 h exposure to cisplatin and [Pt(*O,O′*-acac)(γacac)(DMS)], in both tumour and normal breast epithelial cells in primary culture

Patient number	Normal cisplatin IC_{50} (μM)	Normal [Pt(O,O′-acac)(γ-acac)(DMS)] IC_{50} (μM)	Tumour cisplatin IC_{50} (μM)	Tumour [Pt(O,O′-acac)(γ-acac)(DMS)] IC_{50} (μM)
1	77.0	107.9	100.4	6.5
2	65.3	110.0	94.0	5.0
3	60.1	120.0	90.0	6.2
4	55.4	135.0	103.7	6.6
5	59.3	130.0	98.0	5.5
6	58.0	110.3	93.7	4.2
7	55.9	107.4	94.2	5.0
8	64.4	123.5	94.8	3.8
9	70.1	129.4	94.0	5.8
10	63.0	120.2	101.3	4.3
11	59.2	113.2	99.3	5.1
12	56.8	108.9	87.4	6.0
13	64.8	110.0	82.9	6.2
14	66.0	118.0	104.5	3.5
15	55.4	118.0	107.4	7.1
16	59.0	120.2	95.0	3.7
17	60.3	121.8	94.8	4.1
18	66.8	123.7	97.4	5.7
19	49.9	132.1	99.1	6.2
20	55.2	98.9	90.4	4.4
21	67.4	120.9	94.4	8.0
22	69.1	110.3	97.2	6.0
23	62.0	113.9	98.0	5.1
24	61.2	109.3	107.4	3.8
25	65.4	121.3	105.9	4.0
26	63.9	120.7	93.0	5.1
27	57.4	118.3	93.9	5.9
28	51.9	123.4	103.6	4.0
29	72.1	108.9	82.9	3.5
30	64.7	100.7	80.3	6.4
Mean ± SD	61.9 ± 6.1	116.9 ± 8.8	96.0 ± 6.9	5.22 ± 1.2

cellular accumulation was approximately 17 times higher than that of cisplatin ($P < 0.001$) (Figure 2C). Although the two compounds accumulated in the nucleus with no major differences, the Pt content in DNA bases was considerably higher after treatment with cisplatin than after [Pt(*O,O′*-acac)(γ-acac)(DMS)] thus suggesting that DNA is not the primary target of [Pt(*O,O′*-acac)(γ-acac)(DMS)] in both normal and cancer cells (Figure 2D and E).

Induction of apoptosis by [Pt(O,O′-acac)(γ-acac)(DMS)]

We observed that 100 μmol·L^{-1} of both [Pt(*O,O′*-acac)(γ-acac)(DMS)] and cisplatin resulted in significant cytotoxic effects on both cancer and healthy cells within 24 h of treatment. We therefore used this single concentration of [Pt(*O,O′*-acac)(γ-acac)(DMS)] to study its apoptotic effects. Hallmarks of the apoptotic process include the activation of caspase proteases, which represent both initiators and executors of cell death (Hampton *et al.*, 1998). The cleavage patterns of caspases-3, -7 and -9, caused by various concentrations of [Pt(*O,O′*-acac)(γ-acac)(DMS)] or cisplatin were analysed by Western blotting. PARP cleavage was examined by Western blotting of proteins obtained from isolated nuclei. PARP is one of the first nuclear proteins (113-kDa), which is specifically cleaved by caspases-3 and -7 during apoptosis (Kaufmann *et al.*, 1993).

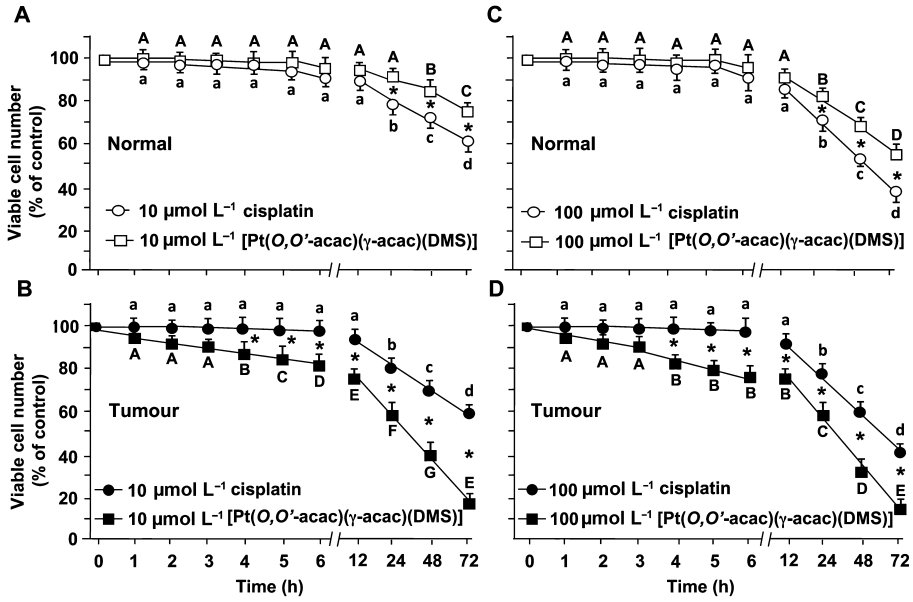

Figure 1

Different dynamics of [Pt(*O,O'*-acac)(γ-acac)(DMS)] and cisplatin effects. Normal (A and C) and tumour (B and D) breast epithelial cells were continuously exposed to 10 or 100 μmol·L^{-1} cisplatin or [Pt(*O,O'*-acac)(γ-acac)(DMS)] and cell viability was monitored by MTT assay over a period of 72 h. The data are means ± SD obtained from 30 different breast cancer cells in primary culture and 30 corresponding normal breast epithelial cells in primary culture, both at passages 2 and 3 and are presented as percentage of control. For cisplatin, $P < 0.0001$ by one-way ANOVA ($n = 30$); values with shared lower case letters are not significantly different according to Bonferroni/Dunn *post hoc* tests. For [Pt(*O,O'*-acac)(γ-acac)(DMS)] $P < 0.0001$ by one-way ANOVA ($n = 30$); values with shared capital letters are not significantly different according to Bonferroni/Dunn *post hoc* tests. *$P < 0.0001$, significant difference between cisplatin and [Pt(*O,O'*-acac)(γ-acac)(DMS)] at the indicated times; unpaired Student's *t*-test.

As shown in Figure 3, in tumour cells, 1 μmol·L^{-1} [Pt(*O,O'*-acac)(γ-acac)(DMS)] significantly increased the amounts of cleaved PARP after 24 h, thus confirming early signs of apoptosis. We observed a PARP fragment (89 kDa) in normal cells treated with 100 μmol·L^{-1} of [Pt(*O,O'*-acac)(γ-acac)(DMS)] and 24 h after treatment (Figure 3). Cisplatin at a concentration of 10 μmol·L^{-1} was sufficient to induce proteolysis of PARP after 24 h in both normal and cancer cells (Figure 3). After 24 h, there was still some full-length PARP detectable, supporting the hypothesis that proteolysis proceeds slowly. Both normal and cancerous cells treated with [Pt(*O,O'*-acac)(γ-acac)(DMS)] did not show activation of caspase-3 (Figure 3A shows the dose–dependent activation of caspases after 24 h). On the other hand, [Pt(*O,O'*-acac)(-acac)(DMS)] caused activation of caspase-7. This activation was fast (3 h) in [Pt(*O,O'*-acac)(γ-acac)(DMS)]-treated tumour cells and slow (24 h) in normal cells (data not shown). The activation of caspase-7 in both normal and cancer cells occurred with 10 μmol·L^{-1} [Pt(*O,O'*-acac)(γ-acac)(DMS)] and was stronger in cancer breast cells (Figure 3A). With regard to caspase-9, known to predominantly activate caspases-3 and -7, we found that the earliest generation of the activated heterodimers occurred after 3 and 24 h in cancer and normal cells respectively (data not shown). Cisplatin caused the activation of caspases-7 and -9 at higher concentrations than [Pt(*O,O'*-acac)(γ-acac)(DMS)] and also caused the activation of caspase-3 (Figure 3A). The inhibition of caspase-3 by siRNA (Figure 3D) provoked a significant decrease in tumour cell death obtained with cisplatin (Figure 3C), while there was no difference in cells treated with [Pt(*O,O'*-acac)(γ-acac)(DMS)] and in normal cells treated with cisplatin (Figure 3B and C), confirming that the apoptotic pathways triggered by the two compounds are different.

Effects of [Pt(O,O'-acac)(γ-acac)(DMS)] and cisplatin on the expression of Bcl-2 family proteins and mitochondrial transmembrane potential in breast cells

Several gene products are known to be important in controlling the apoptotic process. The imbalance of expression of anti- and pro-apoptotic proteins after the stimulus is one of the major mechanisms underlying the ultimate fate of cells in the apoptotic process. Bcl-2 family members, including pro-apoptotic proteins and anti-apoptotic proteins, interact with the mitochondrial outer membrane and function both as a checkpoint upstream of caspases and a mitochondrial gateway (Reed, 2006). In order to investigate whether [Pt(*O,O'*-acac)(γ-acac)(DMS)] and cisplatin induce mitochondrial-mediated apoptosis, the expression levels of pro-apoptotic proteins (Bax and Bid) and anti-apoptotic proteins (Bcl-2) were examined in normal and tumour breast cells.

Exposure of tumour breast cells to [Pt(*O,O'*-acac)(γ-acac)(DMS)] resulted in increased levels of Bax starting at 1 μmol·L^{-1} and simultaneously a significant decreased levels of Bcl-2 (Figure 3A). There was no change in Bcl-2 levels and a less pronounced variation in Bax levels in normal cells using the same experimental. The truncated form of Bid (t-Bid) was

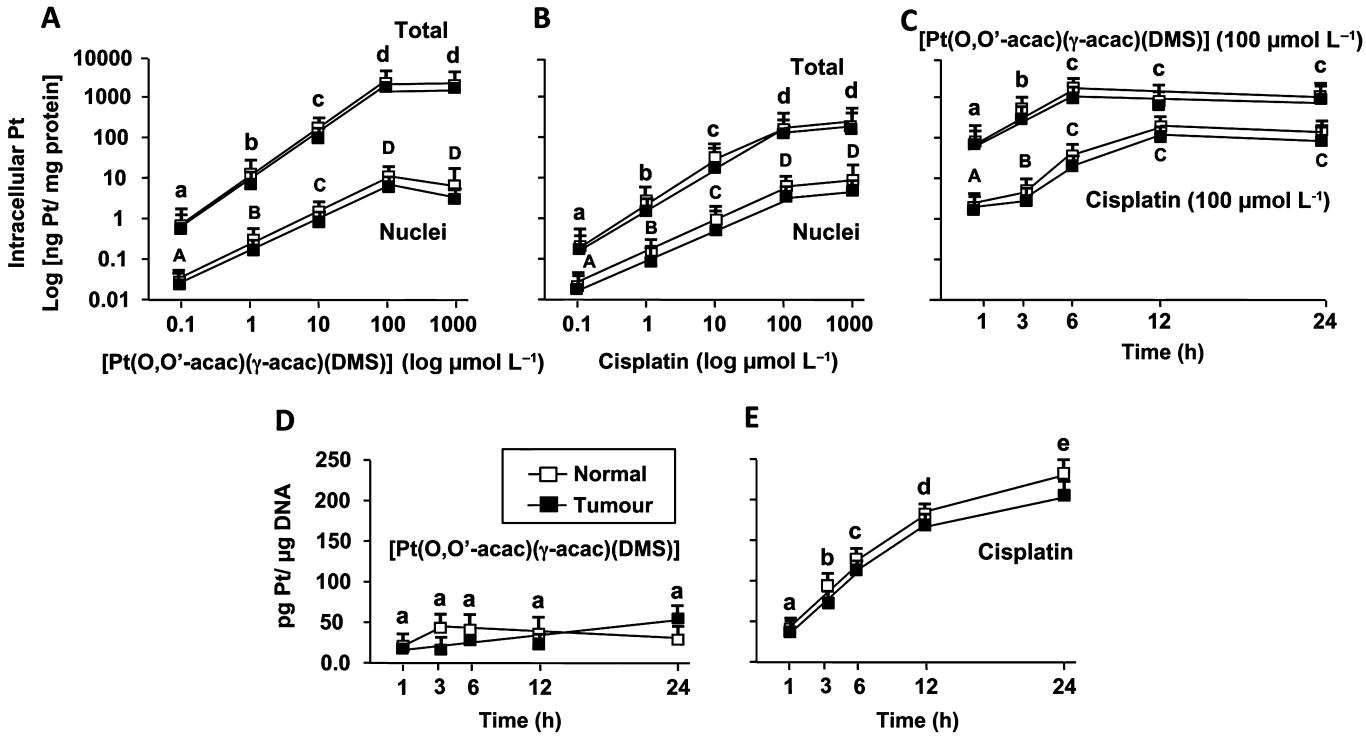

Figure 2

Distribution of Pt in breast cells. Cells were treated with or without increasing concentration of [Pt(*O,O′*-acac)(γ-acac)(DMS)] (A) or cisplatin (B) for 6 h. Cells were treated with or without 100 μmol·L^{-1} [Pt(*O,O′*-acac)(γ-acac)(DMS)] (C and D) or cisplatin (C and E), for the indicated period. Total cellular Pt, nuclear Pt and Pt bound to DNA was determined by atomic absorption spectrometry. Each point represents the means ± SD obtained on a group of five normal and cancer pairs randomly chosen. Statistical analysis was carried out using ANOVA ($n = 5$): (A and B) $P < 0.0001$ for both 'total' and 'nuclei'; (C) $P < 0.0001$ for both [Pt(*O,O′*-acac)(γ-acac)(DMS)] and cisplatin; (D and E) $P > 0.05$ for [Pt(*O,O′*-acac)(γ-acac)(DMS)] and $P < 0.0001$ for cisplatin. Values with shared lower case letters ('total' in A and B and [Pt(*O,O′*-acac)(γ-acac)(DMS)] in C) and values with shared capital letters ('nuclei' in A and B and cisplatin in C) are not significantly different according to Bonferroni/Dunn *post hoc* tests. (A–E) $P > 0.05$ by unpaired Student's *t*-test between normal and tumour cells.

observed only in cancer cells starting at 1 μmol·L^{-1} [Pt(*O,O′*-acac)(γ-acac)(DMS)] (Figure 3A). The effects of cisplatin were more pronounced in normal cells: it increased the expression levels of Bax and decreased the expression levels of Bcl-2. There was no effects on the Bid/t-Bid conversion (Figure 3A).

We determined whether [Pt(*O,O′*-acac)(γ-acac)(DMS)] and cisplatin induced the loss or disruption of mitochondrial transmembrane potential in normal and tumour cells. Mitochondrial membrane depolarization ($\Delta\Psi_m$) was detected fluorimetrically by a shift in fluorescence EM of the cationic lipophilic dye JC-1.

As cellular accumulation of [Pt(*O,O′*-acac)(γ-acac)(DMS)] was approximately 18 times higher than that of cisplatin, we here present data obtained with 5 and 100 μmol·L^{-1} of both [Pt(*O,O′*-acac)(γ-acac)(DMS)] and cisplatin for a better comparison of results.

In tumour cells, $\Delta\Psi_m$ decreased significantly 30 min after addition of [Pt(*O,O′*-acac)(γ-acac)(DMS)] (Figure 4C and D), as determined by mean aggregate fluorescence of JC-1, and reached a minimum after 12 h with both 5 and 100 μmol·L^{-1} of Pt compound. Conversely, $\Delta\Psi_m$ remained high in normal cells and decreased significantly after 24 h of incubation (Figure 4C and D). Differently from [Pt(*O,O′*-acac)(γ-acac)(DMS)], cisplatin treatment (100 μmol·L^{-1}) decreased $\Delta\Psi_m$ significantly only 24 h after incubation in both normal and tumour cells (Figure 4A and B). Mitochondrial fractions were prepared after 15, 30, 60 and 120 min of [Pt(*O,O′*-acac)(γ-acac)(DMS)] treatment. Cytosol-to-mitochondria translocations of Bax and mitochondria-to-cytosol translocations of cytochrome c and Bcl-2 were clearly evident in tumour cells only with both concentrations used (Figure 4E–H).

Effects of [Pt(O,O′-acac)(γ-acac)(DMS)] and cisplatin on the generation of ROS

The effects of [Pt(*O,O′*-acac)(γ-acac)(DMS)] and cisplatin on ROS's levels were 3.5- and 2.5-fold higher for [Pt(*O,O′*-acac)(γ-acac)(DMS)] and cisplatin, respectively, compared with controls (Figure 5A–D). In addition, 5 μmol·L^{-1} [Pt(*O,O′*-acac)(γ-acac)(DMS)] peak was faster (after 7.5 min) compared with 100 μmol·L^{-1} cisplatin (300 min). Furthermore, ROS generation by [Pt(*O,O′*-acac)(γ-acac)(DMS)] was different in normal and cancer cells. No difference was seen in cisplatin-treated cells (Figure 5A–D).

ROS production by [Pt(*O,O′*-acac)(γ-acac)(DMS)] was blocked by both diphenyleneiodonium (DPI), an inhibitor of the NAD(P)H oxidase (Figure 5E) and the antioxidant

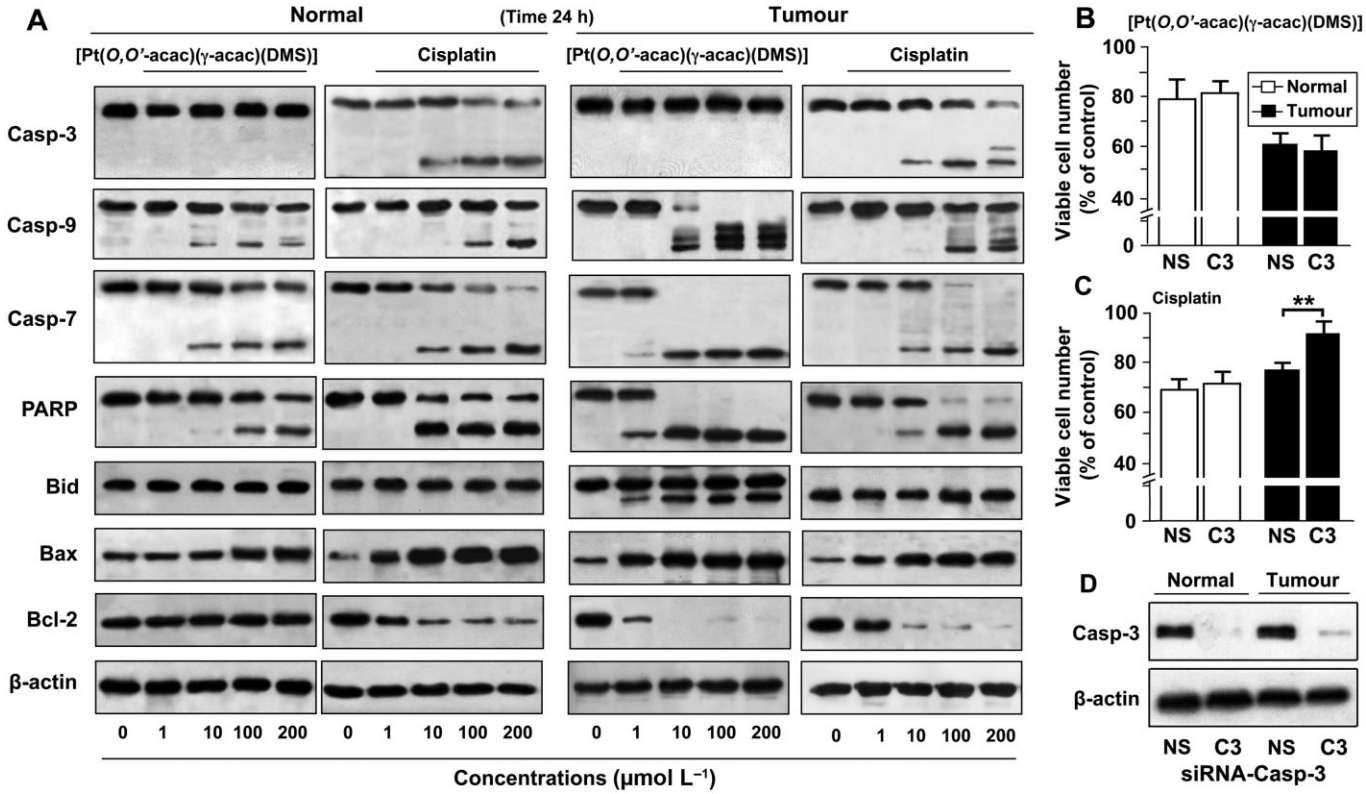

Figure 3

Dose-dependent effect of [Pt(*O,O'*-acac)(γ-acac)(DMS)] and cisplatin on the activation of caspases, the cleavage of PARP and on anti- and proapoptotic proteins. Cytosolic and nuclear proteins were obtained from normal (right panel) and tumour (left panel) breast cells, untreated and treated with increasing concentration of [Pt(*O,O'*-acac)(γ-acac)(DMS)] or cisplatin for 24 h. Samples were dissolved in SDS sample buffer and separated on SDS gel. Immunoblotting was performed using monoclonal anti-PARP, anti-caspases-3, -7 and -9, anti-Bid, anti-Bax and anti-Bcl2. Sequential incubation with anti-β actin confirmed the equal protein loading. These results are representative of five independent experiments carried out on five normal and cancer pairs. (B and C) Viable cell numbers obtained in cells transfected with siRNA-caspase-3 (C3) or with control siRNA (NS), and then incubated with 100 μmol·L^{-1} [Pt(*O,O'*-acac)(γ-acac)(DMS)] (B) or 100 μmol·L^{-1} cisplatin (C) for 24 h. Data are means ± SD (n = 3 normal and cancer pairs randomly chosen). $^{**}P < 0.001$; unpaired Student's t-test. (D) Cells were transfected with siRNA–caspase-3 (C3) or with control siRNA (NS). Cytosolic fraction was separated by SDS–PAGE and analysed by Western blotting using monoclonal anti-caspases-3 antibody. These results are representative of three independent experiments carried out on three normal and cancer pairs. Sequential incubation with anti-β-actin confirmed the equal protein loading.

apocynin, a natural organic compound structurally related to vanillin commonly known as acetovanillone, at a concentration of 10 μg·mL^{-1} (Figure 5E).

Differently from [Pt(*O,O'*-acac)(γ-acac)(DMS)], ROS generation by cisplatin was blocked completely by apocynin, while DPI had no effect (Figure 5F). This suggests the involvement of NAD(P)H oxidase in the [Pt(*O,O'*-acac)(γ-acac)(DMS)]-evoked processes only. As the mithochondria are important sources of intracellular ROS, in order to understand the effects of cisplatin on ROS generation, we studied the specific production of mitochondrial O_2^- by MitoSOX red. We found that cisplatin increased the mitochondrial synthesis of O_2^- in a time-dependent manner (Figure 5H and L) starting approximately after 3 h and reaching a maximum after 10 h. This O_2^- production was blocked by apocynin. It was shown that [Pt(*O,O'*-acac)(γ-acac)(DMS)] also induced a mitochondrial synthesis of O_2^- that became significant approximately after 60 min of incubation, at the time of a considerable decrement of $\Delta\Psi_m$. After 2 h of [Pt(*O,O'*-acac)(γ-acac)(DMS)] treatment, a very high level of fluorescence was observed in cancer cells suggesting a high level of mitochondrial O_2^- production. Apocynin greatly decreased the fluorescence due to [Pt(*O,O'*-acac)(γ-acac)(DMS)] administration (Figure 5G and I).

Discussion

Cisplatin is one of the most potent drugs used for the treatment of various cancers (sarcoma, soft tissue, bones, muscles and blood vessels) (Florea and Büsselberg, 2013). The clinical efficacy of cisplatin has led to a considerable effort to develop its derivatives and other effective metal-based anti-neoplastic compounds (Chen *et al.*, 2009; Che and Siu, 2010; Frezza *et al.*, 2010). The use of cisplatin is limited due to its side effects in normal tissues. Its derivatives, carboplatin and oxaliplatin, have received approval for clinical practice throughout the world. Recent research has focused the

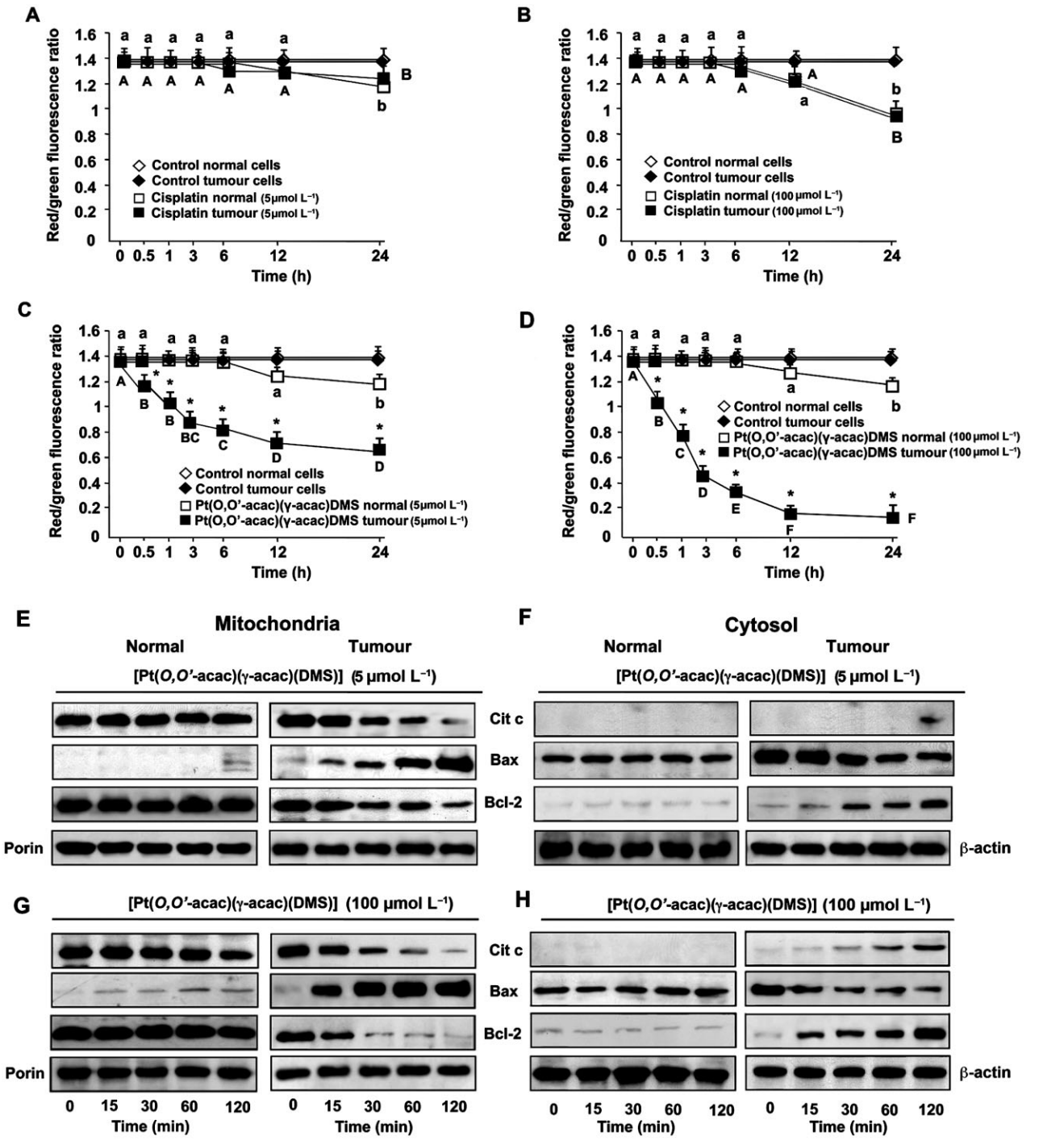

Figure 4

Effect of [Pt(*O,O′*-acac)(γ-acac)(DMS)] and cisplatin on $\Delta\Psi_{m.}$ (A and B) Fluorescent spectra of JC-1 in breast cells treated or not with 5 or 100 μmol·L^{-1} cisplatin or [Pt(*O,O′*-acac)(γ-acac)(DMS)] (C and D) for the indicated time. The data are means ± SD of five different experiments carried out on five normal and cancer pairs and are presented as red J-aggregates/green monomer JC-1 fluorescence ratio. (E and F) Normal and tumour breast cells were treated or not with 5 or 100 μmol·L^{-1} [Pt(*O,O′*-acac)(γ-acac)(DMS)] at the indicated time. Mitochondrial (E) and cytosolic (F) fractions were separated by SDS–PAGE and analysed by Western blotting using monoclonal, anti-cytochrome c, anti-Bid, anti-Bax and anti-Bcl2. Porin and β-actin served as an indicator for mitochondrial and cytosolic extracts respectively. These results are representative of five independent experiments carried out on five normal and cancer pairs. Statistical analysis was carried out using ANOVA ($n = 5$): (A–D) $P > 0.05$ for controls; (A and B) $P < 0.001$ for both normal and tumour cells treated with cisplatin; (C and D) $P < 0.0001$ for both normal and tumour cells treated with [Pt(*O,O′*-acac)(γ-acac)(DMS)]. Values with shared lower case letters (normal cells treated with cisplatin or with [Pt(*O,O′*-acac)(γ-acac)(DMS)]) and values with shared capital letters (tumour cells treated with cisplatin or with [Pt(*O,O′*-acac)(γ-acac)(DMS)]) are not significantly different according to Bonferroni/Dunn *post hoc* tests. (A–D) *$P < 0.0001$, significant difference between normal and tumour cells; unpaired Student's *t*-test.

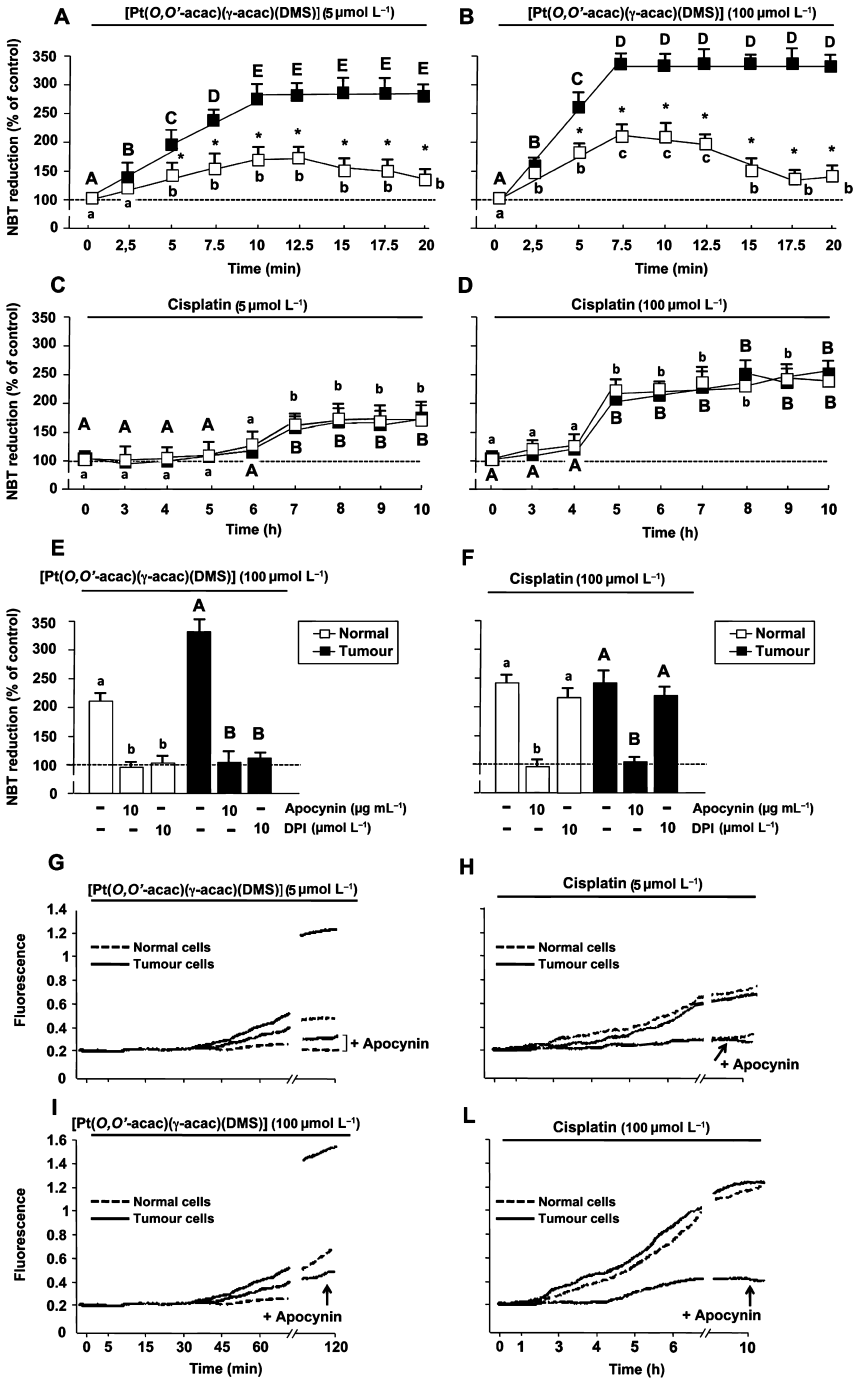

Figure 5

The effect of [Pt(*O,O′*-acac)(γ-acac)(DMS)] and cisplatin on ROS generation. (A–F) Cells preincubated without or with apocynin or DPI for 30 min were exposed to 5 or 100 μmol·L^{-1} [Pt(*O,O′*-acac)(γ-acac)(DMS)] (A, B, E) or cisplatin (C, D, F) for the indicated time intervals. ROS values for [Pt(*O,O′*-acac)(γ-acac)(DMS)] were measured after 7.5 min (E) and after 8 h for cisplatin (F). ROS production was assayed by NBT reduction as described in the Methods section. The data are means ± SD of five independent experiments carried out on five normal/cancer pairs. Statistical analysis was carried out using the ANOVA (n = 5): (A–F) $P < 0.0001$ for normal and tumour cells treated with cisplatin or with [Pt(*O,O′*-acac)(γ-acac)(DMS)]. Values with shared lower case letters (normal cells treated with cisplatin or with [Pt(*O,O′*-acac)(γ-acac)(DMS)]) and values with shared capital letters (tumour cells treated with cisplatin or with [Pt(*O,O′*-acac)(γ-acac)(DMS)]) are not significantly different according to Bonferroni/Dunn *post hoc* tests. (A and B) *$P < 0.001$, significant difference between normal and tumour cells at the indicated times; unpaired Student's *t*-test. (C and D) $P > 0.05$ by unpaired Student's t-test between normal and tumour cells. (G and L) Production of mitochondrial anion superoxide (O^{2-}) was studied by MitoSOX red fluorescence. The fluorescence intensity was measured with a fluorimeter, with EX monochromators setted at 488 nm, with a chopper interval of 0.5 s, and the EM monochromator setted at 580 nm. Arrows (+apocynin) indicate the fluorescence curves obtained when 10 μg/mL apocynin was added to cells.

attention on the synthesis of other Pt anticancer drugs forming DNA adducts or targeting proteins and pathways critical for apoptosis (Lebwohl and Canetta, 1998; De Pascali *et al.*, 2005; 2009; Zhang *et al.*, 2009; Olszewski and Hamilton, 2010; Florea and Büsselberg, 2013). A new Pt(II) complex ([Pt(*O,O′*-acac)(γ-acac)(DMS)]), specific for non-genomic targets, has been designed and synthesized by some of us in order to overcome the cisplatin-related problems (De Pascali *et al.*, 2009). This compound exhibits interesting biological activities and contains two acetylacetonate ligands, one *O,O′*-chelate and the other σ-linked to methionine in the γ position and DMS in the metal coordination sphere (Muscella *et al.*, 2007; 2008; 2010; 2011a,b; De Pascali *et al.*, 2009). While the cytotoxicity of cisplatin appears to be associated both with its intracellular accumulation and the formation of DNA adducts, the cytotoxicity of this new compound is due to its intracellular accumulation only. It shows a low reactivity with nucleobases and a specific reactivity with sulphur ligands, suggesting that the cellular targets could be amino acid residues of proteins. The different mechanism of action of [Pt(*O,O′*-acac)(γ-acac)(DMS)] may render it intrinsically able to evoke less chemoresistance (Muscella *et al.*, 2008). [Pt(*O,O′*-acac)(γ-acac)(DMS)] exhibited higher antitumour activity than cisplatin also in breast cancer cell lines relatively resistant to many chemotherapeutic agents, cisplatin included (Muscella *et al.*, 2008). Recently, a variety of Pt complexes with sulphur ligands were synthesized and analysed (Mügge *et al.*, 2014) and these novel Pt compounds also preferentially induced apoptosis over necrosis.

It is important to determine whether [Pt(*O,O′*-acac)(γ-acac)(DMS)] is specifically toxic to cancer cells. We have studied the effects of [Pt(*O,O′*-acac)(γ-acac)(DMS)] in primary cultured epithelial breast cells obtained from 30 cancer tissues and corresponding histologically proven non-malignant tissue adjacent to the tumour. The cytotoxicity profile of cisplatin was also assessed in the same cells. Our results confirm that [Pt(*O,O′*-acac)(γ-acac)(DMS)] is more potent than cisplatin and its cytotoxic activity is higher in epithelial breast cancer cells than in normal cells in primary culture (Figure 1 and Table 1). This activity indicated that [Pt(*O,O′*-acac)(γ-acac)(DMS)] is a potential novel anti-tumour agent.

[Pt(*O,O′*-acac)(γ-acac)(DMS)] entered the cells quickly and its cellular accumulation was higher than that of cisplatin (Figure 2). The cytotoxic effects of [Pt(O,O′-acac)(γ-acac)(DMS)] were greater than the effects elicited by equal concentrations of cisplatin and were more rapidly expressed (Figure 1). Furthermore, as cellular accumulation of [Pt(*O,O′*-acac)(γ-acac)(DMS)] was approximately 18 times higher than that of cisplatin (Figure 2), this prompted us to use an 18-fold lower concentration of [Pt(*O,O′*-acac)(γ-acac)(DMS)] in further experiments. Despite this, the cytotoxic effects of 5 μmol·L^{-1} [Pt(*O,O′*-acac)(γ-acac)(DMS)] were greater and more rapid in onset than those elicited by 100 μmol·L^{-1} cisplatin (Figures 4 and 5).

Another important point was the different cellular distribution of cisplatin and [Pt(*O,O′*-acac)(γ-acac)(DMS)]. Both compounds accumulated approximately to the same level in the nucleus, but [Pt(*O,O′*-acac)(γ-acac)(DMS)] was rarely bound to the DNA (Figure 2D and E). [Pt(*O,O′*-acac)(γ-acac)(DMS)] cytotoxicity was approximately 18-fold greater than that of cisplatin in cancer cells. Normal cells were significantly less sensitive to [Pt(*O,O′*-acac)(γ-acac)(DMS)]. The cytotoxic effects of [Pt(*O,O′*-acac)(γ-acac)(DMS)] were fast and more pronounced in cancer than in normal cells (Figure 1). Noteworthy, the IC_{50} values obtained with both [Pt(*O,O′*-acac)(γ-acac)(DMS)] and cisplatin did not show much variability (Table 1). As cisplatin shows variability in responses in patients (Petrelli *et al.*, 2014), a higher variability in our cellular experiments could be expected. The reason for this can be twofold: first, tumours used in our study were homogeneous (all infiltrating ductal carcinomas, 87% ER receptor positive and only one sample triple negative); second, cells in primary cultures are deprived of all *in vivo* interactions with the surrounding environment, the immune system and a plethora of biological signals; all these factors may render cultured cells more equally sensitive to the action of the drugs.

Most of the chemotherapeutic agents kill cancer cells by a variety of mechanisms including intercalation into DNA, inhibition of DNA replication, cell membrane damage or free radical generation (Wesselborg *et al.*, 1999). The immediate effect of [Pt(*O,O′*-acac)(γ-acac)(DMS)] in tumour cells is ROS production through the activation of NAD(P)H oxidase (Figure 5). In MCF-7 cells, [Pt(*O,O′*-acac)(γ-acac)(DMS)] increased the synthesis of ROS through both activation of NAD(P)H oxidase and mitochondrial pathways (Muscella *et al.*, 2010), as often observed in the early stages of apoptosis (Kakkar and Singh, 2007). In our experiments, we observed that inhibition of NAD(P)H oxidase completely blocked ROS generation in the first 10 min while cisplatin appeared to activate later on mainly another important source of intracellular ROS, the mitochondrion, as shown by the specific production of mitochondrial O_2^- by MitoSOX red and by the lack of effects of DPI (Figure 5). Thus, the rapid activation of NAD(P)H oxidase already evident after 2.5 min appeared to be a key event in [Pt(*O,O′*-acac)(γ-acac)(DMS)]-mediating apoptosis. Although the primary intracellular targets of these Pt(II) compound are rather distinct, the drug-induced cytotoxicity ultimately leads to a common pathway causing apoptosis. Generally, cells exposed to anticancer drugs display apoptotic alterations such as cell shrinkage, chromatin condensation, internucleosomal DNA fragmentation (Woldemariam and Mandal, 2008). Caspases are also the central executioners of most of the apoptotic pathways that are activated by multiple stimuli. Upstream initiator caspases, such as caspases-8 and -9, are activated early in the apoptotic process and then activate other downstream caspases such as caspases-3 and -7. These caspases are largely responsible for the cleavage of many other cellular proteins leading to apoptosis (Gonzalez *et al.*, 2001). As caspase-3 is considered to be central to the apoptosis machinery (Cohen, 1997; Jänicke *et al.*, 1998), it was surprising that we observed caspase-7 activation, not caspase-3, after [Pt(*O,O′*-acac)(γ-acac)(DMS)] treatment (Figure 3). As caspase-3 knockout mice have normal apoptotic response (Kuida *et al.*, 1996), and deficiency of a caspase member can be compensated by activation of other caspases (Zheng *et al.*, 2000), there may be regulatory mechanisms that preferentially utilize different caspase members in response to apoptotic stimuli. In some cellular contexts also caspase-3 activation may be dispensable. Our novel finding is nevertheless consistent with a report

demonstrating that upon VP-16 treatment, PARP was cleaved by caspase-7, but not caspase-3 (Germain *et al.*, 1999). It is tempting to speculate that caspase-7 may be preferentially activated by certain chemotherapeutic agents. Caspase-3 lacking MCF-7 cells (Blanc *et al.*, 2000) undergo a caspase-7-mediated apoptosis when treated with [Pt(O,O′-acac)(γ-acac)(DMS)] (Muscella *et al.*, 2008). Caspase-7 is closely related to caspase-3 and shows the same synthetic substrate specificity *in vitro* (Wei *et al.*, 2000), suggesting that caspase-3 and -7 possibly have overlapping roles in apoptosis (Riedl *et al.*, 2001). In this work, we demonstrated that caspase-7 was activated in [Pt(*O,O*′-acac)(γ-acac)(DMS)]-treated normal and tumour cells, even though caspase-3 was expressed and indeed activated by cisplatin (Figure 3). Novel Pt compounds with sulphur ligands also induced apoptosis through the activation of caspases 3/7 although unfortunately were not assessed the activities of caspases-3 and -7 separately (Mügge *et al.*, 2014). Consistent with results obtained in immortalized cell lines (Muscella *et al.*, 2008) the procaspase-9 activation occurred together with the generation of the mature form of caspase-7, indicating the involvement of the intrinsic pathway. There was a difference in the time needed to activate procaspase-7/-9 between normal and tumour cells after [Pt(*O,O*′-acac)(γ-acac)(DMS)] treatment. In cancer cells, activation occurred within 6 h and the activity remained elevated whereas, in normal cells, a significant activation occurred only after 12 h (data not shown). PARP synthesizes poly(ADP-ribose) from NAD in response to strand breaking in DNA. PARP cleavage is an early biochemical event during apoptosis (Germain *et al.*, 1999). In our experiments, PARP cleavage was detected after 24 h of 1 μmol·L^{-1} [Pt(*O,O*′-acac)(γ-acac)(DMS)] treatment in accordance with the effect on tumoural cell survival. In normal cells, PARP cleavage was significantly detected after treatment with 100 μmol·L^{-1} [Pt(*O,O*′-acac)(γ-acac)(DMS)] (Figure 3). Therefore, apoptosis is the major pathway of cell death caused by both [Pt(O,O′-acac)(γ-acac)(DMS)] and cisplatin and occurs through events involving caspase activation. The evaluation of condensed chromatin showed an association between degradation of PARP and alteration of chromatin structure faster and more effective after [Pt(O,O′-acac)(γ-acac)(DMS)] than cisplatin treatment.

The permeabilization of mitochondrial membranes is associated with apoptosis. Mitochondrial membrane permeabilization may occur via the control of proapoptotic Bcl-2 family members, and/or by the induction of the mitochondrial permeability transition. These cell death-inducing regulatory mechanisms are ultimately responsive to the bioenergetic status/redox state of mitochondria. During apoptosis the release of cytochrome c from mitochondria into the cytoplasm occurs after the development of the mitochondrial transition pore. Cytochrome c translocated to the cytoplasm and complexes to and oligomerizes apoptosis-activating factor-1, leading to the activation of caspase-9 and the effector caspase cascade (Kroemer *et al.*, 1998). The translocation of cytochrome c to the cytoplasm generally occurs simultaneously with the decrease of $\Delta\Psi_m$ (Kroemer *et al.*, 1998), another marker of subsequent cell death. In [Pt(*O,O*′-acac)(γ-acac)(DMS)]-treated cells a significant decrease in $\Delta\Psi_m$ was already evident after 30 min and matched the release of mitochondrial cytochrome c, the activation of caspase-9 and PARP cleavage (Figure 4). While a decrease in $\Delta\Psi_m$ was observed at the early stage in [Pt(*O,O*′-acac)(γ-acac)(DMS)]-treated cells, in cisplatin-treated cells it occurred after 24 h (Figure 4). At present, the precise connections linking [Pt(*O,O*′-acac)(γ-acac)(DMS)]-mediated apoptosis to the apoptotic death machinery are not known. However, it is clear that most, if not all, apoptotic stimuli from [Pt(*O,O*′-acac)(γ-acac)(DMS)] eventually funnel into the proapoptotic Bcl-2 proteins. Release of proapoptotic factors from mitochondria is controlled by Bcl-2 and Bax, both members of the mitochondrial membrane-associated Bcl-2 family of proteins with opposing effects on cell life and death (Green and Reed, 1998). Overexpression of Bcl-2, an apoptotic inhibitor (Krajewski *et al.*, 1993), was shown to increase cisplatin resistance in a number of experimental models (Zangemeister-Wittke *et al.*, 1998; Miyake *et al.*, 1999; Mese *et al.*, 2000). Bcl-2 overexpression in the mitochondrial outer membrane and the associated up-regulation of glutathione production contribute to MCF-7 cell survival by mechanisms independent of cisplatin inactivation or inhibition of DNA adduct formation (Rudin *et al.*, 2003). The suppression of Bcl-2 expression reverses MCF-7 cell survival (Basma *et al.*, 2005). In contrast, Bax is a proapoptotic factor that translocates from the cytosol to the outer mitochondrial membrane where it can form heterodimers with Bcl-2 protein to form pores and mediate cytochrome c release. We found that [Pt(*O,O*′-acac)(γ-acac)(DMS)] and cisplatin apoptosis was associated with down-regulation of Bcl-2 (Figure 4) and translocation of Bax from the cytosol to the mitochondria. Our data also suggest that Bid is involved in [Pt(*O,O*′-acac)(γ-acac)(DMS)]- (but not cisplatin-) induced apoptosis. On induction of apoptosis, it was demonstrated that Bid is cleaved to generate t-Bid, which translocates to the mitochondria (Kroemer *et al.*, 1998) oligomerizing and triggering the insertion of Bax (Eskes *et al.*, 2000). During [Pt(*O,O*′-acac)(γ-acac)(DMS)]-mediated induction of apoptosis Bid was cleaved in cancer cells, Bax translocated to the mitochondrial fraction and $\Delta\Psi_m$ decreased. In contrast, no cleavage of Bid occurred in cells after cisplatin treatment (Figure 3).

Our current data do not clarify how Bid is activated. However, it is widely believed that activation of Bid requires its cleavage by caspase-8 or other proteases (Degli Esposti, 2002). Moreover, Bid is also able to oligomerize and trigger the insertion of Bax in isolated mitochondria by excitotoxic injury (Eskes *et al.*, 2000). Subsequent changes in phospholipid composition may convert Bid into a t-Bid that is subsequently able to activate Bax and mitochondrial cell death pathways. In addition, a kinase-mediated regulation of Bid activation was also suggested (Degli Esposti, 2002). Bax expression increased markedly in cells exposed to either [Pt(*O,O*′-acac)(γ-acac)(DMS)] or cisplatin (Figure 4). Results from our experiments show that the mechanism for apoptosis is functional in primary cultured breast cells and [Pt(*O,O*′-acac)(γ-acac)(DMS)] is able to activate the mitochondrial pathway. This is particularly important as tumours accumulate mutations that increase their resistance to apoptotic inducers, for example, attenuation of caspase-3 was associated with multidrug acquired resistance (Kojima *et al.*, 1998). Thus, finding new therapeutic agents that induce caspase-3-independent apoptosis may have valuable clinical implications. [Pt(*O,O*′-acac)(γ-acac)(DMS)] may evoke a different

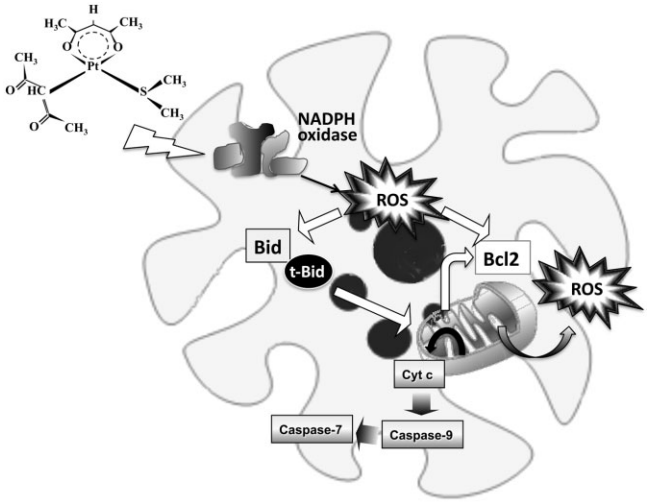

Figure 6

Mechanisms of Pt(*O,O*′-acac)(γ-acac)(DMS)]-induced apoptosis. The effects of Pt(*O,O*′-acac)(γ-acac)(DMS)] in cancer cells are quantitatively different from those obtained in healthy cells. It starts with the generation of ROS by NAD(P)H oxidase and then switch to the activation of the caspase-3-independent apoptotic sequence.

apoptotic pathway from that of oncological drugs such as doxorubicin and etoposide (Yang *et al.*, 2001).

In conclusion, we believe the most interesting data from our experiments are the large difference in cytotoxic response to [Pt(*O,O*′-acac)(γ-acac)(DMS)] between healthy and cancerous cells in all specimens pairs examined. Of great importance is also the difference in cytotoxicity between cisplatin and [Pt(*O,O*′-acac)(γ-acac)(DMS)], especially in relation to healthy cells. Both these observations could predict the intensity of the side effects in normal tissues during Pt(II) clinical use. These differences could be due to the rapid generation of ROS primarily due to the activity of NAD(P)H oxidase by [Pt(*O,O*′-acac)(γ-acac)(DMS)], and the different sequence of molecular events that support the apoptotic process triggered by the two complexes. The key points of this model are summarized in Figure 6.

Acknowledgements

The work presented was supported by the Italian Ministry of Research and University (PRIN 2009: 'Sintesi, caratterizzazione e studio del pathway d'induzione apoptotica di composti antitumorali di Pt per target non genomici').

Author contributions

C. V. and A. M. made the primary culture of breast epithelial cells, performed cytotoxicity assay, Western blotting, siRNA transfection, experiments on ROS generation and assembled data; F. P. F. conceived and supervised the drug design, the synthesis and characterization of Pt compounds; L. G. C. performed spectroscopic analysis of mitochondrial membrane depolarization; D. M. performed Pt determination by ICP-AES spectrometry; S. A. D. P. synthesized and characterized the Pt compounds; S. M. designed all biological experiments, wrote the paper and supervised the study.

Conflict of interest

The authors declare that they have no conflict of interest.

References

Alexander SPH, Benson HE, Faccenda E, Pawson AJ, Sharman JL, Spedding M *et al.* (2013). The Concise Guide to PHARMACOLOGY 2013/14: Enzymes. British J Pharm 170: 1797–1867.

Basma H, El–Refaey H, Sgagias MK, Cowan KH, Luo X, Cheng PW (2005). BCL-2 antisense and cisplatin combination treatment of MCF-7 breast cancer cells with or without functional p53. J Biomed Sci 12: 999–1011.

Blanc C, Deveraux QL, Krajewski S, Janicke RU, Porter AG, Reed JC *et al.* (2000). Caspase-3 is essential for procaspase-9 processing and cisplatin-induced apoptosis of MCF-7 breast cancer cells. Cancer Res 60: 4385–4390.

Cerri S, Piccolini VM, Santin G, Bottone MG, De Pascali SA, Migoni D *et al.* (2011). The developmental neurotoxicity study of platinum compounds. Effects of cisplatin versus a novel Pt(II) complex on rat cerebellum. Neurotoxicol Teratol 33: 273–281.

Che CM, Siu FM (2010). Metal complexes in medicine with a focus on enzyme inhibition. Curr Opin Chem Biol 14: 255–2561.

Chen D, Milacic V, Frezza M, Dou QP (2009). Metal complexes, their cellular targets and potential for cancer therapy. Curr Pharm Des 15: 777–791.

Cohen GM (1997). Caspases: the executioners of apoptosis. Biochem J 326: 1–16.

De Pascali SA, Papadia P, Ciccarese A, Pacifico C, Fanizzi FP (2005). First examples of β-diketonate platinum II complexes with sulfoxide ligands. Eur J Inorg Chem 5: 788–796.

De Pascali SA, Papadia P, Capoccia S, Marchiò L, Lanfranchi M, Ciccarese A *et al.* (2009). Hard/soft selectivity in ligand substitution reactions of β-diketonate platinum (II) complexes. Dalton Trans 77: 86–95.

Degli Esposti M (2002). The roles of Bid. Apoptosis 7: 433–440.

Eskes R, Desagher S, Antonsson B, Martinou JC (2000). Bid induces the oligomerization and insertion of Bax into the outer mitochondrial membrane. Mol Cell Biol 20: 929–935.

Farrell N (1996). Current status of structure–activity relationships of platinum anticancer drugs. Activation of the trans geometry. Met Ions Biol Syst 32: 60–63.

Ferlay J, Shin HR, Bray F, Forman D, Mathers C, Parkin DM (2010). Estimates of worldwide burden of cancer in 2008: GLOBOCAN 2008. Int J Cancer 127: 2893–2917.

Florea AM, Büsselberg D (2013). Breast cancer and possible mechanisms of therapy resistance. JLGHS 2013: 2. doi: 10.5339/jlghs.2013.2

Frezza M, Hindo S, Chen D, Davenport A, Schmitt S, Tomco D *et al.* (2010). Novel metals and metal complexes as platforms for cancer therapy. Curr Pharm Des 16: 1813–1825.

Fuertes MA, Castilla J, Alonso C, Pérez JM (2003). Cisplatin biochemical mechanism of action: from cytotoxicity to induction of cell death through interconnections between apoptotic and necrotic pathways. Curr Med Chem 10: 257–266.

Gandara DR, Wold H, Perez EA, Deisseroth AB, Doroshow J, Meyers F *et al.* (1989). Cisplatin dose intensity in non-small cell lung cancer: phase II results of a day 1 and day 8 high-dose regimen. J Natl Cancer Inst 81: 790–794.

Germain M, Affar EB, D'Amours D, Dixit VM, Salvesen GS, Poirier GG (1999). Cleavage of automodified poly(ADP-ribose) polymerase during apoptosis. Evidence for involvement of caspase-7. J Biol Chem 274: 28379–28384.

Gonzalez VM, Fuertes MA, Alonso C, Perez JM (2001). Is cisplatin-induced cell death always produced by apoptosis? Mol Pharmacol 59: 657–663.

Greco S, Elia MG, Muscella A, Storelli C, Marsigliante S (2002). AT1 angiotensin II receptor mediates intracellular calcium mobilization in normal and tumoural breast cells in primary culture. Cell Calcium 32: 1–10.

Green DR, Reed JC (1998). Mitochondria and apoptosis. Science 281: 1309–1312.

Hampton MB, Zhivotovsky B, Slater AF, Burgess DH, Orrenius S (1998). Importance of the redox state of cytochrome c during caspase activation in cytosolic extracts. Biochem J 329: 95–99.

Jänicke RU, Ng P, Sprengart ML, Porter AG (1998). Caspase-3 is required for alpha-fodrin cleavage but dispensable for cleavage of other death substrates in apoptosis. J Biol Chem 273: 15540–15545.

Kakkar P, Singh BK (2007). Mitochondria: a hub of redox activities and cellular distress control. Mol Cell Biochem 305: 235–253.

Kaufmann SH, Desnoyers S, Ottaviano Y, Davidson NE, Poirier GG (1993). Specific proteolytic cleavage of poly(ADP-ribose) polymerase: an early marker of chemotherapy-induced apoptosis. Cancer Res 53: 3976–3985.

Kojima H, Endo K, Moriyama H, Tanaka Y, Alnemri ES, Slapak CA *et al.* (1998). Abrogation of mitochondrial cytochrome c release and caspase-3 activation in acquired multidrug resistance. J Biol Chem 273: 16647–16650.

Krajewski S, Tanaka S, Takayama S, Schibler MJ, Fenton W, Reed JC (1993). Investigation of the subcellular distribution of the bcl-2 oncoprotein: residence in the nuclear envelope, endoplasmic reticulum, and outer mitochondrial membranes. Cancer Res 53: 4701–4714.

Kroemer G, Dallaporta B, Resche-Rigon M (1998). The mitochondrial death/life regulation in apoptosis and necrosis. Annu Rev Physiol 60: 619–642.

Kuida K, Zheng TS, Na S, Kuan C, Yang D, Karasuyama H *et al.* (1996). Decreased apoptosis in the brain and prematurelethality in CPP32-deficient mice. Nature 384: 368–372.

Lebwohl D, Canetta R (1998). Clinical development of platinum complexes in cancer therapy: an historical perspective and an update. Eur J Cancer 34: 1522–1553.

Mese H, Sasaki A, Alcalde RE, Nakayama S, Matsumura T (2000). Regulation of apoptosis reduction in the cisplatin-resistant A431 cell line by Bcl-2 and CPP32. Chemotherapy 46: 69–76.

Miyake H, Hara I, Yamanaka K, Arakawa S, Kamidono S (1999). Synergistic enhancement of resistance to cisplatin in human bladder cancer cells by overexpression of mutant-type p53 and Bcl-2. J Urol 162: 2176–2181.

Muscella A, Calabriso N, De Pascali SA, Urso L, Ciccarese A, Fanizzi FP *et al.* (2007). New platinum II complexes containing both an *O,O′*-chelated acetylacetonate ligand and a sulfur ligand in the platinum coordination sphere induce apoptosis in HeLa cervical carcinoma cells. Biochem Pharmacol 74: 28–40.

Muscella A, Calabriso N, Fanizzi FP, De Pascali SA, Urso L, Ciccarese A *et al.* (2008). [Pt(O,O′-acac)(γ-acac)(DMS)], a new Pt compound exerting fast cytotoxicity in MCF-7 breast cancer cells via the mitochondrial apoptotic pathway. Br J Pharmacol 153: 34–49.

Muscella A, Calabriso N, Vetrugno C, Urso L, Fanizzi FP, De Pascali SA *et al.* (2010). Sublethal concentrations of the platinum(II) complex [Pt(O,O′-acac)(γ-acac)(DMS)] alter the motility and induce anoikis in MCF-7 cells. Br J Pharmacol 160: 1362–1377.

Muscella A, Calabriso N, Vetrugno C, Fanizzi FP, De Pascali SA, Marsigliante S (2011a). The signalling axis mediating neuronal apoptosis in response to [Pt(O,O′-acac)(γ-acac)(DMS)]. Biochem Pharmacol 81: 1271–1285.

Muscella A, Calabriso N, Vetrugno C, Fanizzi FP, De Pascali SA, Storelli C *et al.* (2011b). The platinum (II) complex [Pt(O,O′-acac)(γ-acac)(DMS)] alters the intracellular calcium homeostasis in MCF-7 breast cancer cells. Biochem Pharmacol 81: 91–103.

Mügge C, Liu R, Görls H, Gabbiani C, Michelucci E, Rüdiger N *et al.* (2014). Novel platinum(II) compounds with O,S bidentate ligands: synthesis, characterization, antiproliferative properties and biomolecular interactions. Dalton Trans 43: 3072–3086.

Olszewski U, Hamilton G (2010). A better platinum-based anticancer drug yet to come? Anticancer Agents Med Chem 10: 293–301.

Pawson AJ, Sharman JL, Benson HE, Faccenda E, Alexander SP, Buneman OP, Davenport AP, McGrath JC, Peters JA, Southan C, Spedding M, Yu W, Harmar AJ; NC-IUPHAR. (2014). The IUPHAR/BPS Guide to PHARMACOLOGY: an expert-driven knowledge base of drug targets and their ligands. Nucl Acids Res 42 (Database Issue): D1098–1106.

Petrelli F, Coinu A, Borgonovo K, Cabiddu M, Ghilardi M, Lonati V *et al.* (2014). The value of platinum agents as neoadjuvant chemotherapy in triple-negative breast cancers: a systematic review and meta-analysis. Breast Cancer Res Treat 144: 223–232.

Reed JC (2006). Proapoptotic multidomain Bcl-2/Bax-family proteins: mechanisms, physiological roles, and therapeutic opportunities. Cell Death Differ 13: 1378–1386.

Riedl SJ, Fuentes-Prior P, Renatus M, Kairies N, Krapp S, Huber R *et al.* (2001). Structural basis for the activation of human procaspase-7. Proc Natl Acad Sci U S A 98: 790–795.

Rudin CM, Yang Z, Schumaker LM, VanderWeele DJ, Newkirk K, Egorin MJ *et al.* (2003). Inhibition of glutathione synthesis reverses Bcl-2-mediated cisplatin resistance. Cancer Res 63: 312–318.

Smiley ST, Reers M, Mottola-Hartshorn C, Lin M, Chen A, Smith TW *et al.* (1991). Intracellular heterogeneity in mitochondrial membrane potentials revealed by a J-aggregate forming lipophilic cation JC-1. Proc Natl Acad Sci U S A 88: 3671–3675.

Smith IE, Talbot DC (1992). Cisplatin and its analogues in the treatment of advanced breast cancer: a review. Br J Cancer 65: 787–793.

Strasser A, Harris AW, Jacks T, Cory S (1994). DNA damage can induce apoptosis in proliferating lymphoid cells via p53-independent mechanisms inhibitable by Bcl-2. Cell 79: 329–339.

Wei Y, Fox T, Chambers SP, Sintchak J, Coll JT, Golec JM *et al*. (2000). The structures of caspases-1, -3, -7 and -8 reveal the basis for substrate and inhibitor selectivity. Chem Biol 7: 423–432.

Wesselborg S, Engels IH, Rossmann E, Los M, Schulze-Osthoff K (1999). Anticancer drugs induce caspase-8/FLICE activation and apoptosis in the absence of CD95 receptor/ligand interaction. Blood 93: 3053–3063.

Woldemariam GA, Mandal SS (2008). Iron(III)-salen damages DNA and induces apoptosis in human cell via mitochondrial pathway. J Inorg Biochem 102: 740–747.

Yang XH, Sladek TL, Liu X, Butler BR, Froelich CJ, Thor AD (2001). Reconstitution of caspase-3 sensitizes MCF-7 breast cancer cells to doxorubicin and etoposide induced apoptosis. Cancer Res 61: 348–354.

Zangemeister-Wittke U, Schenker T, Luedke GH, Stahel RA (1998). Synergistic cytotoxicity of bcl-2 antisense oligodeoxynucleotides and etoposide, doxorubicin and cisplatin on small cell lung cancer cell lines. Br J Cancer 78: 1035–1042.

Zhang J, Wang L, Xing Z, Liu D, Sun J, Li X *et al*. (2009). Status of bi- and multi-nuclear platinum anticancer drug development. Mini Rev Med Chem 9: 1357–1366.

Zheng TS, Hunot S, Kuida K, Momoi T, Srinivasan A, Nicholson DW *et al*. (2000). Deficiency in caspase-9 or caspase-3 induces compensatory caspase activation. Nat Med 6: 1241–1247.